THE INFLUENCE OF SPECIFIC CUTTING FORCE ON END MILLING MODELS

Anna Carla Araujo, José Luís Lopes Silveira

XVI CONGRESSO BRASILEIRO DE ENGENHARIA MECÂNICA
16th BRAZILIAN CONGRESS OF MECHANICAL ENGINEERING

THE INFLUENCE OF SPECIFIC CUTTING FORCE ON END MILLING MODELS

Anna Carla Araujo
PEM/COPPE/UFRJ - P.O. Box 68503 – 21945-970 – Rio de Janeiro, RJ, Brazil.
anna@ufrj.br

José Luís Silveira
PEM/COPPE/UFRJ - P.O. Box 68503 – 21945-970 – Rio de Janeiro, RJ, Brazil.
jluis@ufrj.br

Abstract. *In order to predict machining forces it is necessary to know the chip volume and calculate the specific cutting force of the process, the prediction force problem is concerned on the right formulation of this last parameter that most models considers constant. This paper analyzes the behavior of the specific cutting pressures on end milling by calculating, from experimental data force, the pressure on each moment of cut. This procedure involves an approach which do not considers the force on each cutting edge piece but a function of area and height of cutting. After the cutting pressure analysis, some comparisons with previously published experiments are done and it can be seen that for the prediction of end milling cutting forces, the variation in time of the specific cutting force should be considered.*

Keywords: *specific cutting force, end milling, machining modelling*

1. Introduction

The end milling process is one of the most widely used and efficient means of machining materials. In this process there is a periodically varying chip section during the material removal and the cutting force also varies during this process. Accurate modelling of the cutting forces is required to predict the cutting forces, vibration, surface quality, and stability of machining processes.

A number of different methods to predict cutting forces have been developed over the last years. These models can be classified into three major categories: empirical, analytical, and mechanistic methods. In the empirical methods, a number of machining experiments are performed and performance measures such as cutting forces, tool life, and tool wear are measured (Armarego and Brown, 1969). These responses are then correlated to the cutting conditions using empirical functions and require a lot of experimentation. Analytical approaches, (Armarego and Brown, 1969) and (Altintas, 2000) model the physical mechanisms that occur during cutting. This include complex mechanisms such as high strain rates, high temperature gradients and combined elastic and plastic deformations and it's not yet completely solved. Mechanistic models (Tlusty and MacNeil, 1975; Kline *et all*, 1982; Altintas and Spence, 1991; Yun and Cho, 2001 and Kapoor *et all*, 2001) predict the cutting forces based on a method that assumed cutting force to be proportional to the chip cross-sectional area.

The constants of proportionality are called the specific cutting pressures and depend on the cutter geometry, cutting conditions, insert grade and workpiece material properties. This paper questions the behavior in time of specific cutting pressures for cutting force models for end milling process, estimating the specific cutting pressures directly from cutting force data previously published.

2. Cutting force modelling of end-milling operations

Instantaneous differential force modelling for one single flute is normally written by Martelotti formula (Araujo and Silveira, 1999)

$$d\vec{F_i} = \vec{K}\ dA = \vec{K}\, t\, db \tag{1}$$

where $\vec{K}$ is a vector called specific cutting force and the instantaneous force is the sum of differential parts calculated on small cutting tool pieces (db) multiplied by the specific force and the uncut chip thickness (t) that for end milling can be written as:

$$t = s_t \sin\phi \tag{2}$$

where ϕ is the angle of the cutting piece measured in relation of the normal direction of the feed per tooth s_t,

$$s_t = \frac{v}{\omega\, N_f} \tag{3}$$

from known v, ω and N_f as the feed velocity, rotation velocity and the number of flutes.

The cutting tool pieces can be calculated by

$$db = \frac{d}{2\ \tan\lambda} d\phi \tag{4}$$

where d is the tool diameter and λ is the helix angle. (Fig. (1))

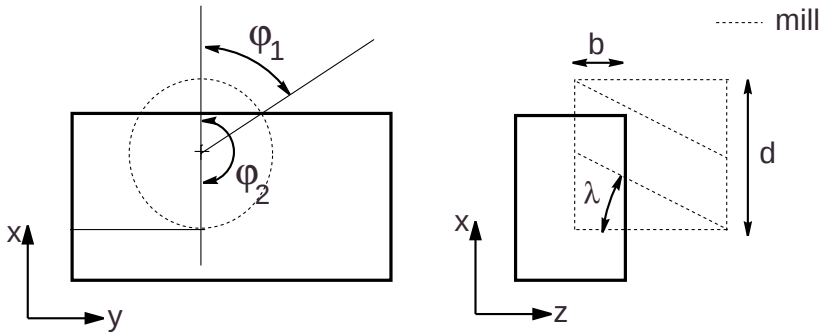

Figure 1. Milling geometry.

The angle δ is calculated by

$$\delta = \frac{2\, b \tan\lambda}{d} \tag{5}$$

where b is the the depth of cut.

The angle δ is used to classify the cutting geometry as *Type I* or *Type II* (Tab. (1)), where φ_1 and φ_2 are the entry and exit angles, respectively (Fig. (1)), which were enlightened on (Tlusty and MacNeil, 1975) and (Araujo and Silveira, 1999).

Table 1. Classification as *Type I* or *Type II*.

Type I	*Type II*
$\delta \leq \varphi_2 - \varphi_1$	$\delta > \varphi_2 - \varphi_1$

The force become:

$$\vec{F_i} = \int \vec{K} dA = \int \vec{K} t db = \int \vec{K}\ \frac{d\, s_t\ \sin\phi}{2\ \tan\lambda}\ d\phi \tag{6}$$

So, the total force of cut, considering the N_f flutes of the mill, are calculated by the sum:

$$\vec{F} = \sum_{i=1}^{N_f} \vec{F_i} \tag{7}$$

In this approach, all force contributions are calculated at the same time because all differential parts of the force are calculated for each cutting piece.

3. Force as a function of time

The milling force vector ($\vec{\mathbf{F}}(t)$) is written as the multiplication of two parcels: one relative to the specific force, written as a vector function ($\vec{\mathbf{K}}(t)$), and other relative to the cutting area, an scalar function ($\mathbf{A}(t)$). This form is called from now on by *Function of area variation approach.*

$$\vec{\mathbf{F}}(t) = \vec{\mathbf{K}}(t)\mathbf{A}(t) \tag{8}$$

The time variable t can be substituted by the angle of rotation θ of a fixed point $\mathbf{P}$ in a peripheral tool and the tool velocity rotation ω: (Fig. (2))

$$\vec{\mathbf{F}}(t) = \tilde{\vec{\mathbf{F}}}\Big(\frac{\theta}{\omega}\Big) = \vec{F}(\theta) \tag{9a}$$

$$\vec{F}(\theta) = \vec{K}(\theta) \quad A(\theta) \tag{9b}$$

The function $A(\theta)$ will be calculated separately in the following section.

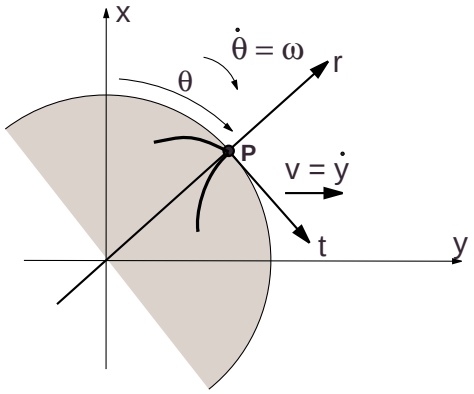

Figure 2. Milling Tool Referential.

4. The Cross-sectional Area Variation

Let take the area parcel separately to construct the area function $\mathbf{A}(\theta)$.

In Fig. (3) can be observed the chip cross-sectional area (A_1) of the first flute at milling angle θ, for a cutting geometry having $\varphi_1 = 0$ and $\varphi_2 = \pi$.

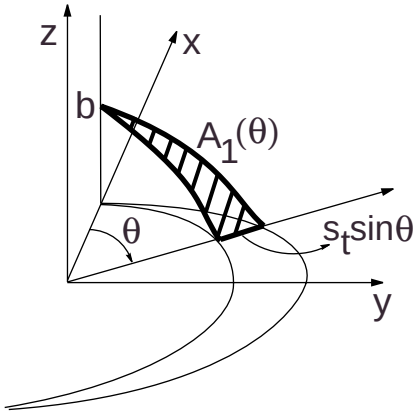

Figure 3. Chip Cross-sectional Area.

The chip area can be calculated by:

$$A_1(\theta) = \int_{L_1(\theta)}^{L_2(\theta)} \frac{s_t\, d}{2\, \sin\lambda} \sin\phi\, d\phi \tag{10}$$

where the limits L_1 and L_2 are functions of θ and are calculated differently for each cutting phase of θ as can be observed on Tab. (2).

Table 2. Integration limits for each phase.

	Type I		Type II	
Phase	$L_1(\theta)$	$L_2(\theta)$	$L_1(\theta)$	$L_2(\theta)$
For $e_1 < \theta \leq e_2$ - Phase A	e_1	θ	e_1	θ
For $e_2 < \theta \leq e_3$ - Phase B	$\theta - \delta$	θ	e_1	e_2
For $e_3 < \theta \leq e_4$ - Phase C	$\theta - \delta$	e_3	$\theta - \delta$	e_2

The values of e_1, e_2, e_3 and e_4 can be extracted from Tab. (3).

Table 3. Variables values.

	Type I	Type II
e_1	φ_1	φ_1
e_2	$\varphi_1 + \delta$	φ_2
e_3	φ_2	$\varphi_1 + \delta$
e_4	$\varphi_2 + \delta$	$\varphi_2 + \delta$

For a single flute and *Type I* cutting geometry, the chip cross-sectional area function is presented on Fig. (4).

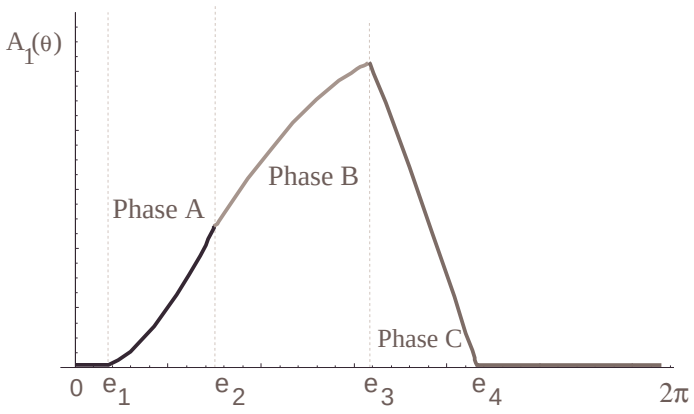

Figure 4. Area Function for one Single Flute.

In order to add the contributions of all flutes, the chip cross-sectional area function for any flute (n) is written by:

$$A_n(\theta) = \int_{L_1(\theta+\xi(n-1))}^{L_2(\theta+\xi(n-1))} \frac{s_t\, d}{2\, \sin\lambda} \sin\varepsilon\, d\varepsilon \tag{11}$$

Note that the functions L_1 and L_2 are now not only a function of θ but also a function of n, where ξ is the angle between the flutes.

The total area is calculated by:

$$A(\theta) = \sum_{n=1}^{N_f} A_n(\theta) \tag{12}$$

and the Fig. (5) shows the chip cross-sectional area function $A(\theta)$ for a milling with four flutes ($\xi = 90^o$) and in bold the function of the first flute $A_1(\theta)$, of a cut having *Type I* geometry.

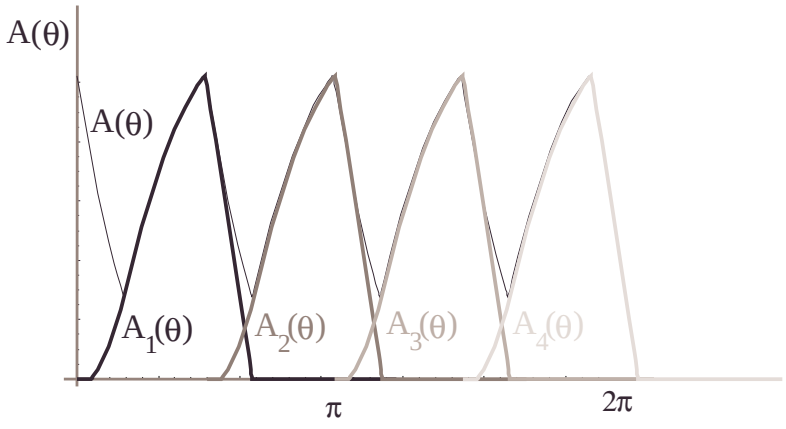

Figure 5. End Milling Area Function.

5. Rotated Area Function

In order to compare the present model with experimental data, the force components should be decomposed in x, y and z directions as they are usually recorded in machining tests.

$$\vec{F}(\theta) = \begin{bmatrix} F_x(\theta) \\ F_y(\theta) \\ F_z(\theta) \end{bmatrix} = A(\theta) \begin{bmatrix} K_x(\theta) \\ K_y(\theta) \\ K_z(\theta) \end{bmatrix} \tag{13}$$

But it's not convenient to write the specific cutting force in the fixed referential x, y, z. To rewrite it on the more appropriate tool referential t, r, z (tangential, radial and axial directions), another function $A_R(\theta)$ has to be introduced:

$$\begin{bmatrix} F_x(\theta) \\ F_y(\theta) \\ F_z(\theta) \end{bmatrix} = A_R(\theta) \begin{bmatrix} K_t(\theta) \\ K_r(\theta) \\ K_z(\theta) \end{bmatrix} \tag{14}$$

In fact, the function $A_R(\theta)$ is the rotation matrix $\mathbf{R}(\theta)$ multiplied by the area.

$$\mathbf{R}(\theta) = \begin{pmatrix} \cos(\theta) & \sin(\theta) & 0 \\ \sin(\theta) & -\cos(\theta) & 0 \\ 0 & 0 & 1 \end{pmatrix} \tag{15}$$

The rotation matrix $\mathbf{R_n}(\theta)$ have to be written for each flute:

$$\mathbf{R_n}(\theta) = \begin{pmatrix} \cos(\theta + \xi\,(n-1)) & \sin(\theta + \xi\,(n-1)) & 0 \\ \sin(\theta + \xi\,(n-1)) & -\cos(\theta + \xi\,(n-1)) & 0 \\ 0 & 0 & 1 \end{pmatrix} \tag{16}$$

Then, for all flutes, the rotated area function becomes:

$$A_R(\theta) = \sum_{n=1}^{N_f} \mathbf{R_n}(\theta)\, A_n(\theta) \tag{17}$$

To simplify the following calculations, $C_1(\theta)$ and $C_2(\theta)$ are defined:

$$C_1(\theta) = \sum_{n=1}^{N_f} A_n(\theta)\, \cos(\theta + \xi\,(n-1)) \tag{18a}$$

$$C_2(\theta) = \sum_{n=1}^{N_f} A_n(\theta)\, \sin(\theta + \xi\,(n-1)) \tag{18b}$$

$$A(\theta) = \sum_{n=1}^{N_f} A_n(\theta) \tag{18c}$$

Rewriting the Eq. (14), the force can be expressed by:

$$\begin{bmatrix} F_x(\theta) \\ F_y(\theta) \\ F_z(\theta) \end{bmatrix} = A_R(\theta) \begin{bmatrix} K_t(\theta) \\ K_r(\theta) \\ K_z(\theta) \end{bmatrix} = \begin{bmatrix} C_1(\theta) & C_2(\theta) & 0 \\ C_2(\theta) & -C_1(\theta) & 0 \\ 0 & 0 & A(\theta) \end{bmatrix} \begin{bmatrix} K_t(\theta) \\ K_r(\theta) \\ K_z(\theta) \end{bmatrix} \tag{19}$$

Multiplying the matrix $A_R(\theta)$ by a fictitious specific cutting force, e.g. $K_t(\theta) = K_r(\theta) = K_z(\theta) = 1N/mm^2$, can be analyzed the contribution only from the area, with constant specific force. (Fig. (6))

$$\begin{bmatrix} f_x(\theta) \\ f_y(\theta) \\ f_z(\theta) \end{bmatrix} = A_R(\theta) \begin{bmatrix} 1 \\ 1 \\ 1 \end{bmatrix} \tag{20}$$

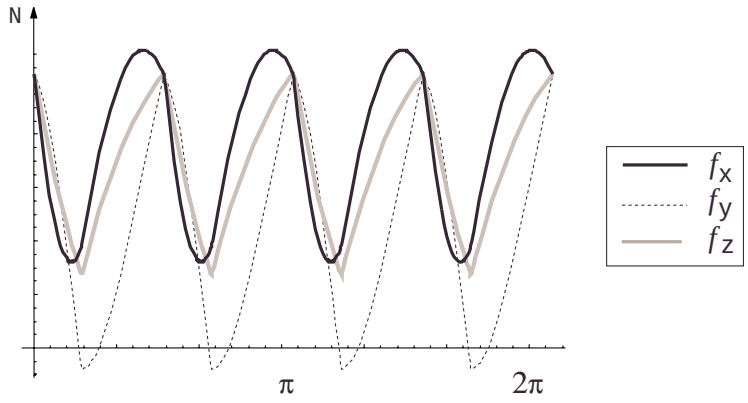

Figure 6. Cutting force for fictitious constant specific force ($K_t(\theta) = K_r(\theta) = K_z(\theta) = 1\ N/mm^2$).

Note that the matrix $A_R(\theta)$ is the Jacobian of the **F** components in relation to the specific cutting force coefficients:

$$A_R(\theta) = \begin{bmatrix} \frac{\partial F_x}{\partial K_t} & \frac{\partial F_x}{\partial K_r} & \frac{\partial F_x}{\partial K_z} \\ \frac{\partial F_y}{\partial K_t} & \frac{\partial F_y}{\partial K_r} & \frac{\partial F_y}{\partial K_z} \\ \frac{\partial F_z}{\partial K_t} & \frac{\partial F_z}{\partial K_r} & \frac{\partial F_z}{\partial K_z} \end{bmatrix} \tag{21}$$

6. Specific Force Analysis

The problem is concentrated on the specific cutting force analysis. The Eq. (19) can be easily calculated if the specific pressure is constant in time (θ).

Empirical works, (Tlusty and MacNeil, 1975) and (Ber *et all*, 1988), considered the specific force as one single value for each pair of tool-workpiece and relate the components by coefficients of proportionality; these researchers considers that the specific force is time constant.

Analytical approaches (Altintas, 2000) calculate the specific cutting forces as a function of cutting parameters.

Orthogonal and Oblique are the most important models and the specific cutting forces are presented on Tab. (4), where ϕ is the shear angle, α the rake angle, β the friction angle, η the chip flow angle, and the "lower index" n means the normal component of the angles.

Table 4. Analytical Specific Force.

	Orthogonal Model	Oblique Model
K_t	$\frac{\tau_s \cos(\beta-\alpha)}{\sin\phi\cos(\phi+\beta-\alpha)}$	$\frac{\tau_s}{\sin\phi_n} \frac{(\cos(\beta_n-\alpha_n)+\tan\lambda\ \tan\eta\ \sin\beta_n)}{\sqrt{\cos^2(\phi_n+\beta_n-\alpha_n)+\tan^2\eta\sin^2\beta_n}}$
K_r	$\frac{\tau_s \sin(\beta-\alpha)}{\sin\phi\cos(\phi+\beta-\alpha)}$	$\frac{\tau_s}{\sin\phi_n} \frac{(\cos(\beta_n-\alpha_n)\tan\lambda-\tan\eta\sin\beta_n)}{\sqrt{\cos^2(\phi_n+\beta_n-\alpha_n)+\tan^2\eta\sin^2\beta_n}}$
K_z	0	$\frac{\tau_s}{\sin\phi_n\cos\lambda} \frac{(\sin(\beta_n-\alpha_n))}{\sqrt{\cos^2(\phi_n+\beta_n-\alpha_n)+\tan^2\eta\sin^2\beta_n}}$

If these parameters are time constant, the specific cutting force will not change in time. To analyze this behavior, for each point of θ, the Eq. (22)

$$\mathbf{K}(\theta) = \mathbf{A_R}^{-1}(\theta)\mathbf{F}(\theta) \tag{22}$$

can be applied to any experimental data from milling process, then if the specific cutting force is constant, the result must has the same value.

The graphic from Fig. (7) was taken from (Altintas and Lee, 1996). This experiment used the following parameters:

$$d = 18.1mm, \quad \lambda = 30.0, \quad N_f = 4, \quad b = 5.08, \quad \varphi_1 = 0, \quad \varphi_2 = \frac{\pi}{2}, \quad v = 30\frac{m}{min}, \quad s_t = 0.05.$$

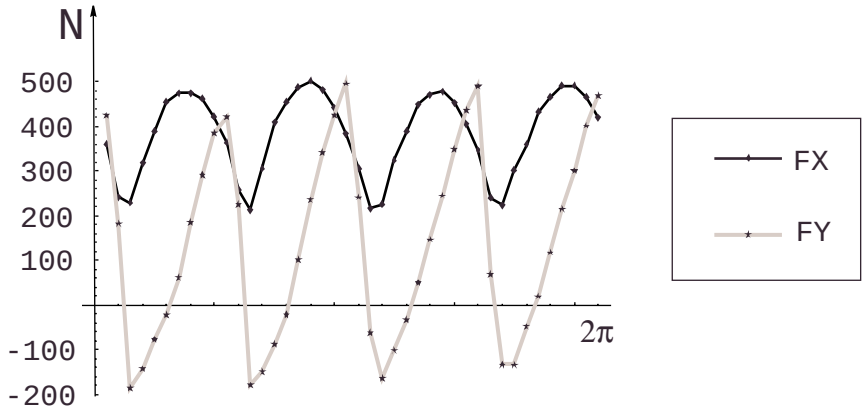

Figure 7. Experimental data from Altintas and Lee (1996).

Taking each point of the curve (Fig. (7)) and calculating the proposed Eq. (22), results in behavior shown in the Fig. (8), that is $K(\theta)$ is not constant:

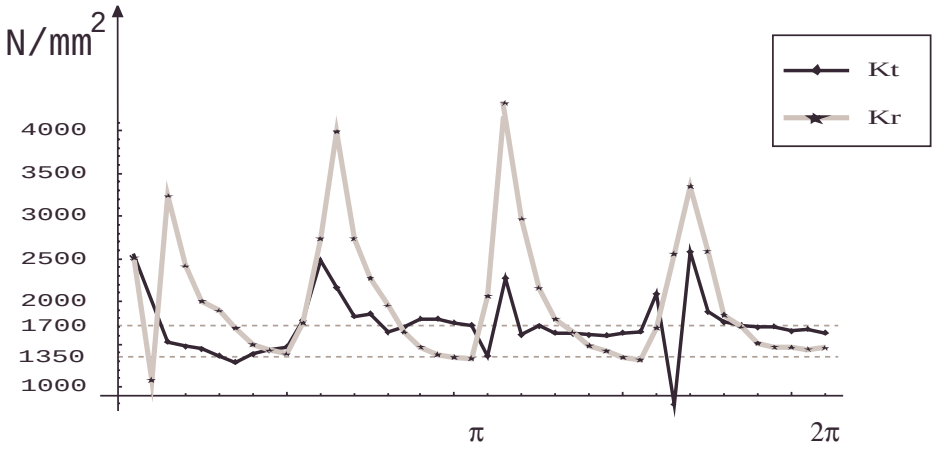

Figure 8. ${A_R}^{-1}\vec{F}$ Graphic.

Analyzing these points, with the aim to get the best proposal for the specific cutting force, the Eq. (19) is recalculated and compared with the experimental data.

The first test is concerned on a constant value: the mean of the function presented in Fig. (8):

$$K_{tmedio} = \frac{1}{p}\sum_{i=1}^{p} K_t(\theta) \tag{23a}$$

$$K_{rmedio} = \frac{1}{p}\sum_{i=1}^{p} K_r(\theta) \tag{23b}$$

where p is the number of points.

Those values, applied on Eq. (19) produces the forces presented and compared with the experimental data in Fig. (10).

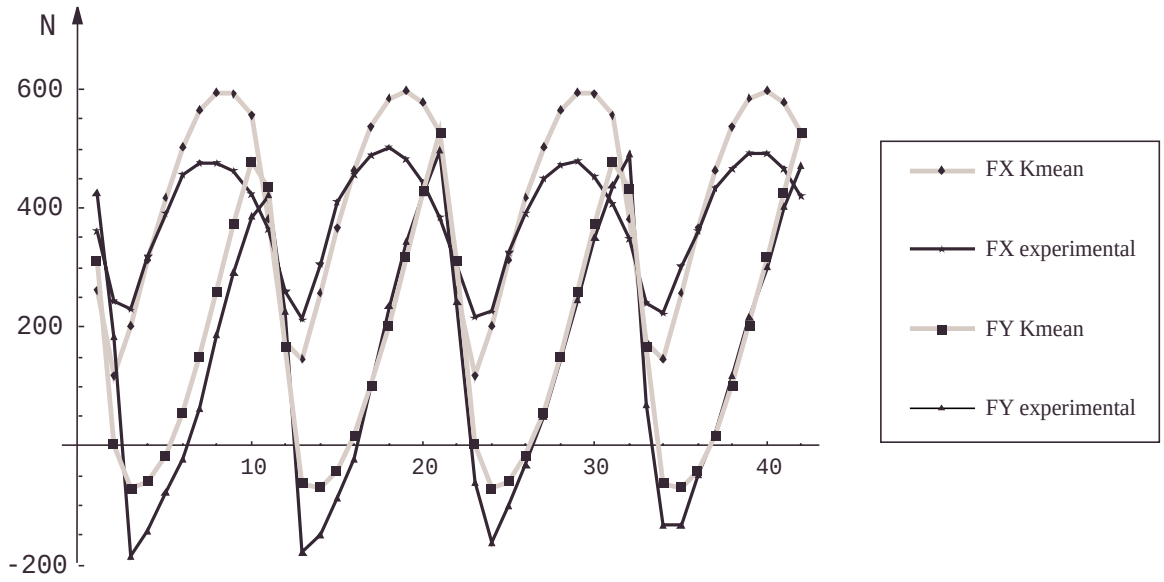

Figure 10. Comparison between experimental force and the force calculated from the mean specific force.

To improve the value of the constant specific force, those who minimize the difference between the theoretical and experimental forces are the asymptotic values: (Fig. (8))

$$K_{tconstant} = 1700\ N/mm^2 \qquad K_{rconstant} = 1350\ N/mm^2 \tag{24}$$

Applied on Eq. (19) results the comparison presented in Fig. (11):

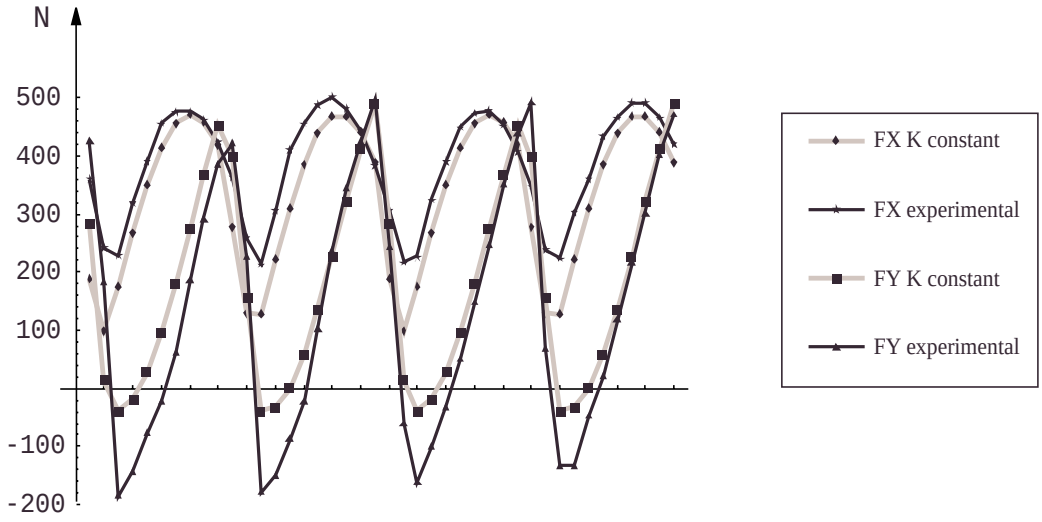

Figure 11. Comparison between experimental force and the force calculated from a constant specific force.

So, constant values for the specific force do not produces good agreement with the experiment.

In a mechanistic approach, one proposal is modelling the radial specific force as a function of the cross-sectional area, because it varies with θ.

Here, the proposed function for the radial specific cutting force is:

$$K_{rvariable} = k_{r1}\ A(\theta)^{-1}\ +\ k_{r2} \tag{25}$$

where $k_{r1} = 240\ N/mm^4$ and $k_{r2} = 500\ N/mm^2$. (Fig. (12))

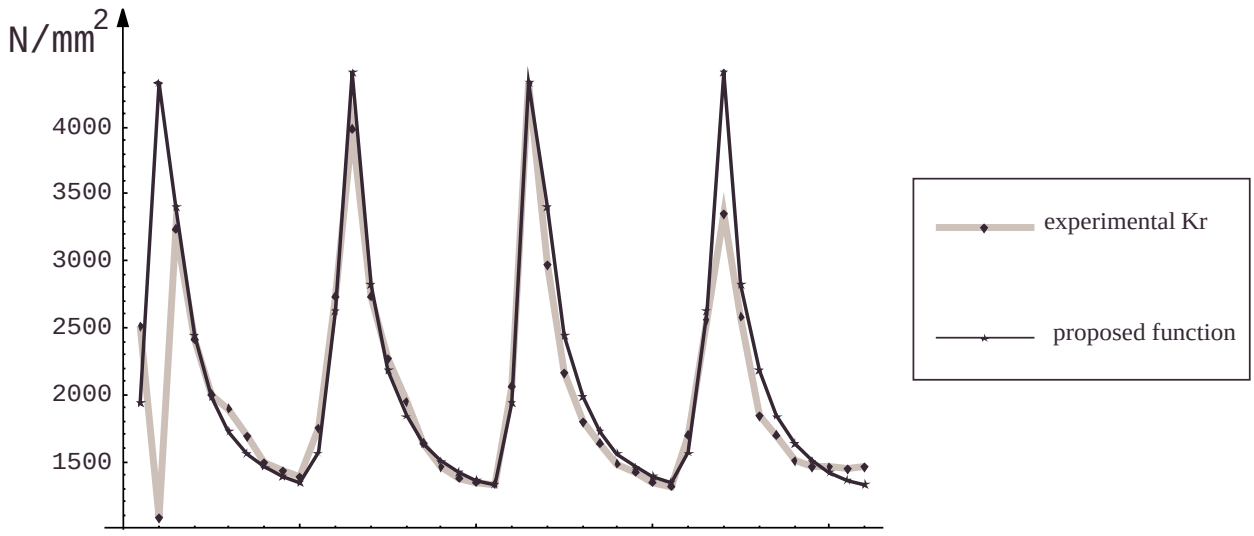

Figure 12. Proposed function for radial specific cutting force.

Using this proposal for the radial specific force and the tangential asymptotic value ($K_t = 1700\ N/mm^2$) and applying on Eq. (19):

$$\begin{bmatrix} F_x(\theta) \\ F_y(\theta) \\ F_z(\theta) \end{bmatrix} = \begin{bmatrix} C_1(\theta) & C_2(\theta) & 0 \\ C_2(\theta) & -C_1(\theta) & 0 \\ 0 & 0 & A(\theta) \end{bmatrix} \begin{bmatrix} K_t \\ k_{r1}\, A(\theta)^{-1} + k_{r2} \\ K_z \end{bmatrix} \tag{26}$$

The Fig. (13) presents the comparison of the result of the Eq. (26) with the experiment. For this case, can be observed that the cutting force model with time variable cutting pressure is more precise then the constant specific force.

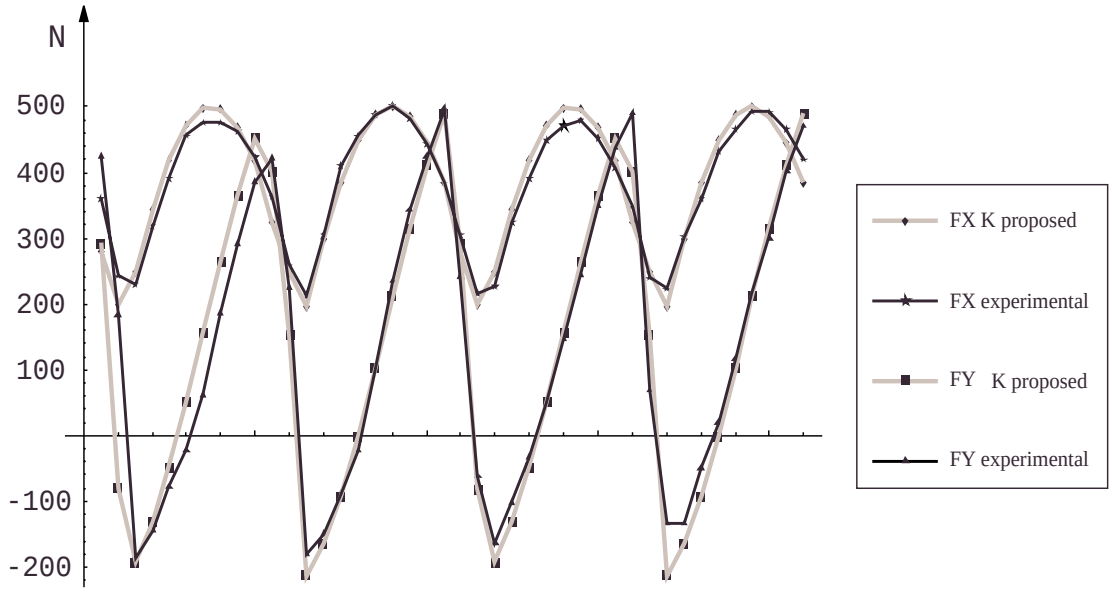

Figure 13. Comparison between experimental and calculated force from proposed specific force function.

Applying on Eq. (19) and rewriting, the Eq. (28) becomes:

$$\begin{bmatrix} F_x(\theta) \\ F_y(\theta) \\ F_z(\theta) \end{bmatrix} = A_R(\theta) \begin{bmatrix} K_t \\ k_{r2} \\ K_z \end{bmatrix} + k_{r1} \begin{bmatrix} C_2(\theta)\, A(\theta)^{-1} \\ -C_1(\theta)\, A(\theta)^{-1} \\ 0 \end{bmatrix} \tag{27}$$

and shows that, for this case, the problem is engaged.

7. Conclusions

This paper analyzes the behavior of the specific cutting pressures from experimental cutting force data. A procedure to estimate the specific cutting forces from data is developed using the function of area variation approach. The developed method is validated by recalculation of the cutting force and compared with the experiment published by (Altintas and Lee, 1996). From the results, it can be seen that the prediction of end milling forces should consider the variation on time of the specific cutting force.

8. Acknowledgements

This research was partially supported by FUJB (Fundação Universitária José Bonifácio) under project 8451-4.

9. References

Altintas, U., 2000, "Manufacturing Automation", Cambridge University Press, 1st edition.

Altintas, U. and Lee, P., 1996, "A General Mechanics and Dynamics Model for Helical End Mills", Annals of CIRP, Vol.45/1, pp. 59-64.

Altintas, U. and Spence, A., 1991,"End Milling force algorithm for CAD Systems", Annals of CIRP, Vol.40/1, pp. 31-34.

Araujo, A.C. and Silveira,J.L., 1999,"Models for the Prediction of Instantaneous Cutting Forces in End Milling", Annals of 15th COBEM, CDROM.

Armarego, E. and Brown, J., 1969, "The Machining of Metals", Prentice-Hall, New Jersey.

Ber, A., Rotberg, J. and Zombach, 1988, "A Method for Cutting Forces in End Milling", Annals of CIRP, Vol. 37/1, pp. 37-40.

Jayaram, S., Kapoor, S. and DeVor, R., 2001, "Estimation of the Specific Cutting Pressures for Mechanistic Cutting Force Models", Int. J. Mach. Tool. Man., Vol.41, pp. 265-281.

Kline, W., DeVor, R. and Lindberg, J., 1982, "The Prediction of Cutting Forces in End Milling", Int. J. Mach. Tool. Des. Res., Vol.22/1, pp. 7-22.

Tlusty, J. and MacNeil, P., 1975, "Dynamics of Cutting in End Milling", Annals of the CIRP, Vol.24/1, pp. 213-221.

Yun, W.S., Cho, D.W., 2001,"Accurate 3-D cutting force prediction using cutting condition independent coefficients in end milling", Int. J. Mach. Tool. Man., Vol.41, pp. 463-478.